



**HAL**  
open science

# A new parametric measure of functional dissimilarity: Bridging the gap between the Bray-Curtis dissimilarity and the Euclidean distance

Carlo Ricotta, Sandrine Pavoine

## ► To cite this version:

Carlo Ricotta, Sandrine Pavoine. A new parametric measure of functional dissimilarity: Bridging the gap between the Bray-Curtis dissimilarity and the Euclidean distance. *Ecological Modelling*, 2022, 466, pp.109880. 10.1016/j.ecolmodel.2022.109880 . hal-03766745

**HAL Id: hal-03766745**

**<https://hal.science/hal-03766745>**

Submitted on 1 Sep 2022

**HAL** is a multi-disciplinary open access archive for the deposit and dissemination of scientific research documents, whether they are published or not. The documents may come from teaching and research institutions in France or abroad, or from public or private research centers.

L'archive ouverte pluridisciplinaire **HAL**, est destinée au dépôt et à la diffusion de documents scientifiques de niveau recherche, publiés ou non, émanant des établissements d'enseignement et de recherche français ou étrangers, des laboratoires publics ou privés.

# A new parametric measure of functional dissimilarity: bridging the gap between the Bray-Curtis dissimilarity and the Euclidean distance

Carlo Ricotta<sup>1,\*</sup>, Sandrine Pavoine<sup>2</sup>

<sup>1</sup>Department of Environmental Biology, University of Rome 'La Sapienza', Rome, Italy; <sup>2</sup>Centre d'Ecologie et des Sciences de la Conservation (CESCO), Muséum National d'Histoire Naturelle, CNRS, Sorbonne Université, Paris, France.

\*Corresponding author. E-mail: [carlo.ricotta@uniroma1.it](mailto:carlo.ricotta@uniroma1.it)

**Abstract.** Community ecologists usually consider the Euclidean distance inappropriate to explore the multivariate structure of species abundance data. This is because the Euclidean distance may lead to the counter-intuitive result for which two sample plots with no species in common may be more similar to each other than two plots that share the same species list. To overcome this paradoxical situation, the species abundances need to be normalized in some way. Among the many coefficients used by ecologists for the analysis of assemblage data, the Bray-Curtis dissimilarity is certainly the most commonly used. This measure entails normalization of species-wise differences between two plots by the total species abundance in both plots. By highlighting the relationship between the Bray-Curtis dissimilarity and the Euclidean distance, we propose a parametric dissimilarity measure that is appropriate for handling data on community composition. We also show how the new parametric measure can be generalized to the measurement of functional dissimilarity between two plots. A small dataset on the species functional turnover along a chronosequence on Alpine grasslands is used to illustrate the behavior of the proposed measure.

**Keywords:** Branching requirement; Complementarity; Dissimilarity profile; Species abundances; Species commonness.

## 1. Introduction

Ecologists frequently use multivariate dissimilarity measures between pairs of sampling units (or plots, quadrats, sites, etc.) for investigating the ecological processes that drive community assembly. Many authors have proposed a set of guidelines to help navigate the multitude of existing dissimilarity coefficients for the analysis of ecological data (e.g. Gower and Legendre 1986; Podani 2000; Legendre and De Cáceres 2013; Lengyel and Botta-Dukát 2021). However, selecting an appropriate question-specific coefficient is not always a simple operation.

In this framework, the Euclidean distance is a natural benchmark for assessing any other dissimilarity coefficient because it corresponds to the standard notion of distance in our everyday

37 physical world (Podani 2000). Given two plots  $U$  and  $V$ , let  $x_{Uj}$  and  $x_{Vj}$  be the abundances of  
38 species  $j$  ( $j = 1, 2, \dots, N$ ) in both plots. The Euclidean distance between  $U$  and  $V$  is defined as:

39

$$40 \quad E = \sqrt{\sum_{j=1}^N (x_{Uj} - x_{Vj})^2} \quad (1)$$

41

42 Note that in this paper we generally use the term distance for all measures that have metric  
43 properties; otherwise, the term dissimilarity is used (see Gower and Legendre 1986).

44 In multivariate analysis of assemblage data, a well-known limitation of the Euclidean distance,  
45 which is usually known as the ‘Orlóci paradox’, is that two plots with no species in common may  
46 result more similar than two plots which share the same species (Orlóci 1978). This counter-  
47 intuitive situation occurs because with the Euclidean distance differences in species abundances are  
48 much more relevant than agreement in species presences and absences (Ricotta and Podani 2017).  
49 Accordingly, an important prerequisite for any meaningful measure of community dissimilarity is  
50 what Clarke et al. (2006) have termed ‘complementarity’. This means that the measure reaches its  
51 maximum value when two plots have no species in common.

52 To overcome the ‘Orlóci paradox’ we need to normalize the species abundances in some way. The  
53 dissimilarity coefficient of Bray and Curtis (1957), one of the most popular measures of  
54 multivariate dissimilarity in community ecology, entails normalization of species-wise differences  
55 in  $U$  and  $V$  by the total species abundance in both plots:

56

$$57 \quad D = \frac{\sum_{j=1}^N |x_{Uj} - x_{Vj}|}{\sum_{j=1}^N (x_{Uj} + x_{Vj})} \quad (2)$$

58

59 The Bray-Curtis dissimilarity thus calculates the fraction of the total species abundances in which  
60 the two plots differ.

61 The aim of this paper is twofold: first, by highlighting the relationship between the Euclidean  
62 distance and the Bray-Curtis dissimilarity, we propose a parametric formulation of Eq. 2 that is  
63 adequate for handling species absolute abundances. Next, we will show how this new parametric  
64 measure can be further generalized to summarize the functional dissimilarity between two plots. A  
65 worked example with data on the species functional turnover along a chronosequence on Alpine  
66 grasslands is used to show the behavior of this new measure.

67 **2. Methods**

68 **2.1. A new parametric measure of dissimilarity**

69 We start by observing that the Euclidean distance is the second order ( $\alpha = 2$ ) of the Minkowski  
70 parametric distance:

71

$$72 \quad M^\alpha = \sqrt[\alpha]{\sum_{j=1}^N |x_{Uj} - x_{Vj}|^\alpha} \quad (3)$$

73

74 Unlike the Euclidean and the Bray-Curtis coefficients which are single-point pictures of community  
75 dissimilarity, the Minkowski distance provides a vector description of the differences in species  
76 abundance between  $U$  and  $V$ . For  $\alpha \geq 1$ , the Minkowski distance is a metric, thus conforming to the  
77 triangle inequality (see Gower and Legendre 1986).

78 In the formulation of the Minkowski distance, the parameter  $\alpha$  is related to the distinctness between  
79 sampling units, such that increasing the value of  $\alpha$  increases the relevance of large differences in  
80 species abundances between  $U$  and  $V$  compared to small differences. For  $\alpha$  tending to infinity,  $M^\infty$   
81 tends to  $\max |x_{Uj} - x_{Vj}|$ . As a result, parametric dissimilarity can be thought of as a scaling process  
82 that occurs in abstract data space of species abundances (Podani 1992).

83 By setting  $\alpha = 1$  in Eq. 3, we obtain the Manhattan (or city-block) distance:

84

$$85 \quad M^1 = \sum_{j=1}^N |x_{Uj} - x_{Vj}| \quad (4)$$

86

87 which is the sum of absolute differences in species abundances between  $U$  and  $V$ .  
88 From Eq. 2 and 4, it follows that the Bray-Curtis dissimilarity is nothing else than the Manhattan  
89 distance normalized by the total abundance of all species in both plots:

90

$$91 \quad D = \frac{\sum_{j=1}^N |x_{Uj} - x_{Vj}|}{\sum_{j=1}^N (x_{Uj} + x_{Vj})} = \frac{M^1}{\sum_{j=1}^N (x_{Uj} + x_{Vj})} \quad (5)$$

92

93 This provides a direct connection between the Bray-Curtis dissimilarity and the Minkowski  
94 parametric family. For species abundance data  $x_{Uj}$ , the observation that the Bray-Curtis  
95 dissimilarity is essentially a normalized version of the first order Minkowski distance can be  
96 generalized to the entire parametric family in one of two ways:

97

$$D^\alpha = \frac{\sqrt[\alpha]{\sum_{j=1}^N |x_{Uj} - x_{Vj}|^\alpha}}{\sqrt[\alpha]{\sum_{j=1}^N (x_{Uj} + x_{Vj})^\alpha}} = \sqrt[\alpha]{\frac{\sum_{j=1}^N |x_{Uj} - x_{Vj}|^\alpha}{\sum_{j=1}^N (x_{Uj} + x_{Vj})^\alpha}} \quad (6a)$$

99

100 or, since  $\sum_{j=1}^N (x_{Uj} + x_{Vj}) = \sum_{j=1}^N x_{Uj} + \sum_{j=1}^N x_{Vj}$

101

$$\Delta^\alpha = \frac{\sqrt[\alpha]{\sum_{j=1}^N |x_{Uj} - x_{Vj}|^\alpha}}{\sqrt[\alpha]{\sum_{j=1}^N x_{Uj}^\alpha + \sum_{j=1}^N x_{Vj}^\alpha}} = \sqrt[\alpha]{\frac{\sum_{j=1}^N |x_{Uj} - x_{Vj}|^\alpha}{\sum_{j=1}^N x_{Uj}^\alpha + \sum_{j=1}^N x_{Vj}^\alpha}} \quad (6b)$$

103

104 For  $\alpha = 1$ , Eq. 6a and 6b both recover the Bray-Curtis dissimilarity, while for  $\alpha = 2$  we obtain two  
105 equally admissible normalized versions of the classical Euclidean distance:

$$106 \quad D^2 = \sqrt{\sum_{j=1}^N (x_{Uj} - x_{Vj})^2} / \sqrt{\sum_{j=1}^N (x_{Uj} + x_{Vj})^2} \quad \text{and} \quad \Delta^2 = \sqrt{\sum_{j=1}^N (x_{Uj} - x_{Vj})^2} / \sqrt{\sum_{j=1}^N x_{Uj}^2 + \sum_{j=1}^N x_{Vj}^2},$$

107 respectively. Eq. 6a and 6b thus represent two normalized expressions of the Minkowski distance in  
108 the range  $[0,1]$  that conform to the complementarity requirement. If  $U$  and  $V$  have no species in

109 common  $D^\alpha$  and  $\Delta^\alpha$  are both equal to 1, whereas if for all  $N$  species  $x_{Uj} = x_{Vj}$ , we have

$$110 \quad D^\alpha = \Delta^\alpha = 0.$$

111 Note that the so-called Minkowski inequality:  $\sqrt[\alpha]{\sum_{j=1}^N |x_{Uj} - x_{Vj}|^\alpha} \leq \sqrt[\alpha]{\sum_{j=1}^N x_{Uj}^\alpha} + \sqrt[\alpha]{\sum_{j=1}^N x_{Vj}^\alpha}$  could also  
112 be used to construct a parametric family of normalized dissimilarities

113

$$114 \quad L^\alpha = \frac{\sqrt[\alpha]{\sum_{j=1}^N |x_{Uj} - x_{Vj}|^\alpha}}{\sqrt[\alpha]{\sum_{j=1}^N x_{Uj}^\alpha} + \sqrt[\alpha]{\sum_{j=1}^N x_{Vj}^\alpha}} \quad (6c)$$

115

116 This measure has been previously proposed by Yuan et al. (2016) to quantify the biodiversity  
117 turnover from species relative abundances. However, unlike  $D^\alpha$  or  $\Delta^\alpha$ , Eq. 6c does not always  
118 assign maximum dissimilarity (i.e.  $L^\alpha = 1$ ) to a pair of completely distinct assemblages with no  
119 species in common.

120 **2.2. Extending the measure to functional differences between plots**

121 Functional differences between species are usually represented by a  $N \times N$  matrix of pairwise  
 122 dissimilarities  $d_{ij}$  between species  $i$  and  $j$  such that  $d_{ij} = d_{ji}$  and  $d_{ii} = 0$ . If  $d_{ij}$  is bounded in the  
 123 range  $[0,1]$ , a corresponding functional similarity coefficient can be easily derived as the  
 124 complement of  $d_{ij}$  (i.e.  $s_{ij} = 1 - d_{ij}$ ).

125 According to Leinster and Cobbold (2012), the functional abundance/commonness of species  $j$  in  
 126 plot  $U$  can be defined as the abundance of all species in  $U$  that are functionally similar to  $j$   
 127 (including  $j$  itself):

128

$$129 \quad c_{Uj} = \sum_{i=1}^N x_{Ui} s_{ij} \quad (7)$$

130

131 Therefore, assuming that species with similar traits are likely to support similar functions (Villéger  
 132 et al. 2013),  $c_{Uj}$  summarizes the abundance of all individuals in plot  $U$  that support the functions  
 133 associated with species  $j$ . For details, see Pavoine and Ricotta (2019). If all species in  $U$  are  
 134 maximally dissimilar from  $j$  such that  $s_{ij} = 0$  for all  $i \neq j$ , we have  $c_{Uj} = x_{Uj}$ , meaning that the  
 135 abundance of all species similar to  $j$  cannot be less than the abundance of  $j$  itself. At the other  
 136 extreme, if all species are functionally identical to  $j$  such that  $s_{ij} = 1$ , we have  $c_{Uj} = \sum_{j=1}^N x_{Uj}$  (i.e.  
 137 the total species abundance in plot  $U$ ).

138 In principle, we can thus derive a family of parametric measures of functional dissimilarity between  
 139 plots by substituting in Eq. 6a and 6b the species abundances  $x_{Uj}$  with their commonness  $c_{Uj}$  :

140

$$141 \quad F^\alpha = \sqrt[\alpha]{\frac{\sum_{j=1}^N |c_{Uj} - c_{Vj}|^\alpha}{\sum_{j=1}^N (c_{Uj} + c_{Vj})^\alpha}} \quad (8a)$$

142  
 143 and

144

$$145 \quad \Phi^\alpha = \sqrt[\alpha]{\frac{\sum_{j=1}^N |c_{Uj} - c_{Vj}|^\alpha}{\sum_{j=1}^N c_{Uj}^\alpha + \sum_{j=1}^N c_{Vj}^\alpha}} \quad (8b)$$

146

147 where the summation is taken over all species that are actually present in at least one of the two  
 148 plots (i.e. over all species for which  $x_{Uj} + x_{Vj} > 0$ ).

149 Eq. 8a and 8b provide a parametric version of the Bray-Curtis dissimilarity that includes functional  
 150 differences between species. However, this solution is not entirely satisfactory for two main  
 151 reasons: first, most researchers usually try to assess how the species functional strategies are  
 152 apportioned within the plots, irrespective of the species absolute abundances in each plot (Ricotta et  
 153 al. 2021a). This aspect can be adjusted by calculating functional dissimilarity from the species  
 154 *relative* abundances  $p_{Uj}$  instead of absolute abundances  $x_{Uj}$ . In this case, species commonness  
 155 becomes:

$$157 \quad \omega_{Uj} = \sum_{i=1}^N p_{Ui} s_{ij} \quad (9)$$

158  
 159 thus representing the *relative* abundance of all species in plot  $U$  that are functionally similar to  $j$   
 160 with  $p_{Uj} = x_{Uj} / \sum_{i=1}^N x_{Ui}$  and  $0 \leq \omega_{Uj} \leq 1$ .

161 Second, Eq. 8a and 8b do not conform to the requirement that dissimilarity remains unchanged if  
 162 two species that are functionally identical in every way are merged into a single species (Leinster  
 163 and Cobbold 2012; Pavoine and Ricotta 2019). The essence of this branching requirement is that a  
 164 measure of functional dissimilarity should be able to highlight differences in ecosystem functioning  
 165 between sampling units regardless of the species that sustain these functions. For throughout  
 166 discussion of this aspect, see Leinster and Cobbold (2012); Botta-Dukát (2018); Ricotta et al.  
 167 (2021a).

168 According to Pavoine and Ricotta (2019), this additional aspect can be fixed by multiplying all  
 169 terms of the summations in Eq. 8a and 8b by a species-specific weighting factor

$$171 \quad \lambda_j = \frac{(p_{Uj} + p_{Vj})}{\sum_{j=1}^N (p_{Uj} + p_{Vj})} = \frac{1}{2} (p_{Uj} + p_{Vj}) \quad (10)$$

172  
 173 which represents the pooled abundance of species  $j$  in  $U$  and  $V$  relative to the total species  
 174 abundance in both plots.

175 Therefore, by substituting the species absolute abundances  $x_{Uj}$  with their relative abundances  $p_{Uj}$   
 176 and by introducing the weighting factors  $\lambda_j$  in the calculation of parametric dissimilarity, we can

177 derive two parametric measures that conform to our intuitive notion of functional dissimilarity  
 178 better than the previous ones:

179

$$180 \quad f^\alpha = \sqrt[\alpha]{\frac{\sum_{j=1}^N \lambda_j |\omega_{Uj} - \omega_{Vj}|^\alpha}{\sum_{j=1}^N \lambda_j (\omega_{Uj} + \omega_{Vj})^\alpha}} \quad (11a)$$

181

182 and

183

$$184 \quad \varphi^\alpha = \sqrt[\alpha]{\frac{\sum_{j=1}^N \lambda_j |\omega_{Uj} - \omega_{Vj}|^\alpha}{\sum_{j=1}^N \lambda_j \omega_{Uj}^\alpha + \sum_{j=1}^N \lambda_j \omega_{Vj}^\alpha}} \quad (11b)$$

185

186 Both measures conform to the requirement that the functional dissimilarity between  $U$  and  $V$   
 187 remains unchanged if two species in  $U$  or  $V$  that are functionally identical in every way are merged  
 188 into a single species. In addition, if  $s_{ij} = 0$  for all  $i \neq j$  and  $\lambda_j = 1/N$  for all  $N$  species in the  
 189 assemblage, Eq. 11a and 11b recover their abundance-based versions  $D^\alpha$  and  $\Delta^\alpha$ , respectively.

190

### 191 3. Worked example

192 In this paper, data on Alpine vegetation sampled by Caccianiga et al. (2006) along a  
 193 chronosequence at the foreland of the Rutor glacier (northern Italy) were used. The same data were  
 194 also used by Ricotta et al. (2021a) to investigate the behavior of a different parametric measure of  
 195 functional dissimilarity. This allows us to compare our results with those of Ricotta et al. (2021a).  
 196 The data set (available in Ricotta et al. 2016: Appendix S2) is composed of a community  
 197 composition matrix with the abundances of 45 species collected in 59 plots. The size of each plot  
 198 was approximately 25 m<sup>2</sup>; all species abundances were measured with a five-point ordinal scale  
 199 transformed to ranks. Based on the age of the moraine ridges, plots were assigned to three distinct  
 200 successional stages: early successional vegetation (ESV, 17 plots), mid successional vegetation  
 201 (MSV, 32 plots), and late successional vegetation (LSV, 10 plots).

202 Six functional traits available in Caccianiga et al. (2006) related to the species global spectrum of  
 203 form and function (Diaz et al. 2016) were used: leaf dry matter content (LDMC; %), leaf dry weight  
 204 (LDW; mg), specific leaf area (SLA; mm<sup>2</sup> × mg<sup>-1</sup>), leaf carbon content (LCC; %), leaf nitrogen  
 205 content (LNC; %), and canopy height (CH; mm). First, the traits were linearly rescaled to zero  
 206 mean and unit standard deviation. Next, the scaled traits were used to calculate a matrix of



207 functional Euclidean distances  $d_{ij}$  between the 45 species in the data set. The Euclidean distances  
208 were finally normalized in the unit range by dividing each distance by the maximum value in the  
209 distance matrix.

210 To compute parametric dissimilarity, the species abundances of all plots within each stage were  
211 averaged and the species relative abundances within each stage were computed. The species relative  
212 abundances within each stage were then used, together with the functional distances, to compute the  
213 parametric dissimilarity between the three successional stages according to Eq. 11a and 11b. To this  
214 end, a new R script available in the Supporting information (Appendix 1 and 2) has been produced.

215 The dissimilarity profiles of  $f^\alpha$  vs.  $\alpha$  for  $\alpha > 0$  among the three successional stages are shown in  
216 Figure 1. The profiles of  $\varphi^\alpha$  are very similar to those of  $f^\alpha$ . Therefore, they are shown in Appendix  
217 1. Caccianiga et al. (2006) and Ricotta et al. (2020) showed that the different successional stages of  
218 the chronosequence are characterized by a gradual substitution of ruderal species by stress tolerator  
219 species. From a functional viewpoint, this pattern is associated to a progressive reduction of leaf  
220 nitrogen content and specific leaf area and a corresponding increase of leaf carbon content and leaf  
221 dry matter.

222 These functional differences are mirrored by the dissimilarity profiles of the three successional  
223 stages: in good agreement with Ricotta et al. (2021a), the dissimilarity profiles between the  
224 intermediate stages of the chronosequence (ESV vs. MSV and MSV vs. LSV) show less  
225 pronounced functional differences, whereas the largest functional differences are shown by the  
226 dissimilarity profile between the early and the late successional stages of the Alpine vegetation  
227 (ESV vs. LSV). By increasing the values of the parameter  $\alpha$ , these differences tend to become  
228 increasingly larger, thus showing that the dominant species in the successional stages at the  
229 opposite ends of the chronosequence tend to be functionally well distinct from each other.

230 One of the criticisms sometimes levelled at the Minkowski parametric distance is that, for  $\alpha > 2$ , it  
231 is highly influenced by large species-wise differences, which is not always justified. However, in  
232 Figure 1 we can see that the dissimilarity profiles reach a plateau for values of  $\alpha$  far beyond this  
233 threshold. Therefore, the dissimilarity values calculated for  $\alpha > 2$  carry an important amount of  
234 ecological information on the pattern of functional differences between the dominant species in  
235 different sampling units. This pattern would be overlooked if the calculation of the dissimilarity  
236 profiles were limited to lower values of  $\alpha$ .

237

#### 238 **4. Discussion**

239 In this paper, we introduced a new parametric measure of community dissimilarity that extends the  
240 normalization method inherent in the Bray-Curtis dissimilarity to the whole Minkowski parametric

241 family. Parametric dissimilarity has been used in community ecology for a long time (e.g. Grassle  
242 and Smith 1976; Jost 2007; Chao et al. 2014; Chao and Ricotta 2019) and its use is due to the  
243 consciousness that no single index is able to adequately summarize all facets of the multivariate  
244 dissimilarity among sampling units. Therefore, one uses a parametric family of dissimilarity  
245 measures whose members have increasing sensitivities to large species-wise differences between  
246 plots for increasing values of the selected scale parameter. With parametric functions, such as  $D^\alpha$   
247 or  $\Delta^\alpha$ , dissimilarity can be plotted against the corresponding scale parameter and the resulting  
248 profiles can be compared for the various communities under study (Taillie 1979).

249 A desirable property of  $D^\alpha$  and  $\Delta^\alpha$  is that for both measures, a few characteristic values of the  
250 parameter  $\alpha$  recover more traditional dissimilarity coefficients. For example, for  $\alpha=1$  both  
251 parametric functions reduce to the Bray-Curtis dissimilarity, while for  $\alpha=2$ , two normalized  
252 versions of the classical Euclidean distance,  $D^2$  and  $\Delta^2$ , are obtained. Therefore,  $D^\alpha$  and  $\Delta^\alpha$  are  
253 not just a mere addition to the dissimilarity measures already available in the ecologist's toolbox.  
254 Rather, an interesting novelty of this work is that such measures provide an explicit relationship  
255 between the Bray-Curtis dissimilarity and the Minkowski family that can be further extended to the  
256 measurement of functional dissimilarity. Hence, by providing a unifying perspective for a number  
257 of seemingly unrelated dissimilarity coefficients, both parametric measures help organize different  
258 aspects of species resemblance into a higher-order coherent framework. For a detailed analysis of  
259 the relationships between the newly proposed parametric measures of community dissimilarity and  
260 a number of classical single-point measures of resemblance, see Appendix 3.

261 Note that the normalized Euclidean distances  $D^2$  and  $\Delta^2$  are both S-decomposable, meaning that  
262 their squared values can be additively decomposed into species-level contributions (Ricotta et al.  
263 2021b). Accordingly, with  $D^2$  and  $\Delta^2$  we can decompose the within- and between-group  
264 components of distance-based multivariate ANOVA into additive species-level values. In this way,  
265 we are able to identify the species that contribute most to the compositional differentiation among  
266 the various groups of plots (Ricotta et al. 2021b).

267 By substituting the species abundances  $x_{uj}$  with their commonness  $\omega_{uj}$ , parametric dissimilarity  
268 can be generalized to account for functional differences among species. Unlike most of the  
269 functional dissimilarity measures published to date (e.g. Cardoso et al. 2014; Chao et al. 2014; Chiu  
270 and Chao 2014; Pavoine and Ricotta 2014), the resulting parametric measures  $f^\alpha$  and  $\varphi^\alpha$  are not  
271 based on Whittaker's (1972) classical model of diversity decomposition into alpha, beta and gamma  
272 components. Therefore, they can be calculated from virtually any available interspecies  
273 dissimilarity measure without restrictions on their geometrical properties (for additional details, see

274 e.g. Pavoine and Ricotta 2014). This high flexibility in the choice of the interspecies dissimilarity  
275 coefficients is a desirable aspect of the proposed framework.

276 If the interspecies dissimilarities  $d_{ij}$  are in the range  $[0,1]$ , the corresponding similarities  
277  $s_{ij} = 1 - d_{ij}$  can be interpreted as the fuzzy degree of functional compatibility of species  $i$  with  
278 species  $j$ . Likewise, the commonness of species  $j$ ,  $\omega_{Uj} = \sum_{i=1}^N p_{Ui} s_{ij}$  can be seen as the mean fuzzy  
279 compatibility of all species in  $U$  with species  $j$  (including  $j$  itself). Since most parametric and non-  
280 parametric functional dissimilarity and diversity measures are calculated from interspecies  
281 dissimilarities, this relationship opens the way for a more general mathematical description of  
282 biodiversity in terms of fuzzy set theory (Cross and Sudkamp 2002; Feoli 2018).

283 To conclude, while how to summarize functional dissimilarity remains an open question, we think  
284 that the major advantage of parametric measures is that by comparing different pairs of plots by  
285 their dissimilarity profiles, it is possible to trace how dissimilarity changes as a function of the scale  
286 parameter  $\alpha$ . This operation may help understanding the effects of large and small species-wise  
287 differences on ecological processes in a more general way than by simply using a scalar measure.

288 A familiar problem related to the differential weighting of large and small species-wise differences  
289 for different values of the parameter  $\alpha$  is that two dissimilarity profiles can cross, such that we  
290 cannot unambiguously say which of the two profiles shows the largest functional differences  
291 (Ricotta et al. 2021a). In this paper, we used numerical simulations to show that this is also the case  
292 for the newly proposed parametric measures  $f^\alpha$  and  $\varphi^\alpha$ .

293 This potential inconsistency in the ordering of two parametric profiles was at the basis of Hurlbert's  
294 (1971) critique on the 'nonconcept' of diversity. However, as emphasized by Patil and Taillie  
295 (1982) and Leinster and Cobbold (2012), inconsistent ordering is a common problem in multivariate  
296 analysis and should not be the case for undue pessimism. On the contrary, when two dissimilarity  
297 profiles cross, the positions of the intersections provide relevant ecological information on the  
298 compositional and functional differences between the communities under scrutiny.

299 We thus hope that in spite of all its biological and statistical complexity, this work will help awaken  
300 some interest to parametric dissimilarity functions and their ecological applications.

- 301 **References**
- 302 Botta-Dukát, Z. (2018) The generalized replication principle and the partitioning of functional  
303 diversity into independent alpha and beta components. *Ecography* 41: 40–50.
- 304 Bray, J., Curtis, J. (1957) An ordination of the upland forest communities in southern Wisconsin.  
305 *Ecological Monographs* 27: 325–349.
- 306 Caccianiga, M., Luzzaro, A., Pierce, S., Ceriani, R.M., Cerabolini, B. (2006) The functional basis of  
307 a primary succession resolved by CSR classification. *Oikos* 112: 10–20.
- 308 Cardoso, P., Rigal, F., Carvalho, J.C., Fortelius, M., Borges, P.A.V., Podani, J., Schmera, D. (2014)  
309 Partitioning taxon, phylogenetic and functional beta diversity into replacement and richness  
310 difference components. *Journal of Biogeography* 41: 749–761.
- 311 Chao, A., Chiu, C.H., Jost, L. (2014) Unifying species diversity, phylogenetic diversity, functional  
312 diversity, and related similarity and differentiation measures through Hill numbers. *Annual*  
313 *Review of Ecology, Evolution, and Systematics* 45: 297–324.
- 314 Chao, A., Ricotta, C. (2019) Quantifying evenness and linking it to diversity, beta diversity, and  
315 similarity. *Ecology* 100: e02852.
- 316 Chiu, C.H., Chao, A. (2014) Distance-based functional diversity measures and their decomposition:  
317 a framework based on Hill numbers. *PLOS ONE* 9: e100014.
- 318 Clarke, K.R., Somerfield, P.J., Chapman, M.G. (2006) On resemblance measures for ecological  
319 studies, including taxonomic dissimilarities and a zero-adjusted Bray-Curtis coefficient for  
320 denuded assemblages. *Journal of Experimental Marine Biology and Ecology* 330: 55–80.
- 321 Cross, V.V., Sudkamp, T.A. (2002) *Similarity and Compatibility in Fuzzy Set Theory*. Physica  
322 Verlag, Heidelberg.
- 323 Díaz, S., Kattge, J., Cornelissen, J.H.C., Wright, I.J., Lavorel, S. et al. (2016) The global spectrum  
324 of plant form and function. *Nature* 529: 167–171.
- 325 Feoli, E. (2018) Classification of plant communities and fuzzy diversity of vegetation systems.  
326 *Community Ecology* 19: 186–198.
- 327 Gower, J.C., Legendre, P. (1986) Metric and Euclidean properties of dissimilarity coefficients.  
328 *Journal of Classification* 3: 5–48.
- 329 Grassle, J.F., Smith, W. (1976) A similarity measure sensitive to the contribution of rare species  
330 and its use in investigation of variation in marine benthic communities. *Oecologia* 25: 13–22.
- 331 Hurlbert, S.H. (1971) The nonconcept of species diversity: a critique and alternative parameters.  
332 *Ecology* 52: 577–586.
- 333 Jost, L. (2007) Partitioning diversity into independent alpha and beta components. *Ecology* 88:  
334 2427–2439.
- 335 Legendre, P., De Cáceres, M. (2013) Beta diversity as the variance of community data: dissimilarity  
336 coefficients and partitioning. *Ecology Letters* 16: 951–963.
- 337 Leinster, T., Cobbold, C.A. (2012) Measuring diversity: the importance of species similarity.  
338 *Ecology* 93: 477–489.
- 339 Lengyel, A., Botta-Dukát, Z. (2021) Review and performance evaluation of trait-based between-  
340 community dissimilarity measures. *bioRxiv*, doi: <https://doi.org/10.1101/2021.01.06.425560>
- 341 Orlóci, L. (1978) *Multivariate Analysis in Vegetation Research*. Junk, The Hague.
- 342 Patil, G.P., Taillie, C. (1982) Diversity as a concept and its measurement. *Journal of the American*  
343 *Statistical Association* 77: 548–561.
- 344 Pavoine, S., Ricotta, C. (2014) Functional and phylogenetic similarity among communities.  
345 *Methods in Ecology and Evolution* 5: 666–675.
- 346 Pavoine, S., Ricotta, C. (2019) Measuring functional dissimilarity among plots: Adapting old  
347 methods to new questions. *Ecological Indicators* 97: 67–72.
- 348 Podani, J. (1992) Space series analysis: processes reconsidered. *Abstracta Botanica* 16: 25–29.
- 349 Podani, J. (2000) *Introduction to the Exploration of Multivariate Biological Data*. Backhuys,  
350 Leiden, NL.

- 351 Ricotta, C., Acosta, A.T.R., Caccianiga, M., Cerabolini, B.E.L., Godefroid, S., Carboni, M. (2020)  
352 From abundance-based to functional-based indicator species. *Ecological Indicators* 118: 106761.  
353 Ricotta, C., de Bello, F., Moretti, M., Caccianiga, M., Cerabolini, B., Pavoine, S. (2016) Measuring  
354 the functional redundancy of biological communities: a quantitative guide, *Methods in Ecology*  
355 *and Evolution* 7: 1386–1395.  
356 Ricotta, C., Pavoine, S., Cerabolini, B.E.L., Pillar, V. (2021b) A new method for indicator species  
357 analysis in the framework of multivariate analysis of variance. *Journal of Vegetation Science* 32:  
358 e13013.  
359 Ricotta, C., Podani, J. (2017) On some properties of the Bray-Curtis dissimilarity and their  
360 ecological meaning. *Ecological Complexity* 31: 201–205.  
361 Ricotta, C., Szeidl, L., Pavoine, S. (2021a) Towards a unifying framework for diversity and  
362 dissimilarity coefficients. *Ecological Indicators* 129: 107971.  
363 Taillie, C. (1979) Species equitability: a comparative approach. In: Grassle, J.F., Patil, G.P., Smith,  
364 W.K., Taillie, C. (Eds.), *Ecological Diversity in Theory and Practice*. International Cooperative  
365 Publishing House, Fairland, MD, pp. 51–62.  
366 Villéger, S., Grenouillet, G., Brosse, S. (2013) Decomposing functional  $\beta$ -diversity reveals that low  
367 functional  $\beta$ -diversity is driven by low functional turnover in European fish assemblages. *Global*  
368 *Ecology and Biogeography* 22: 671–681.  
369 Whittaker, R. (1972) Evolution and measurement of species diversity. *Taxon* 21: 213–251.  
370 Yuan, Y., Buckland, S.T., Harrison, P.J., Foss, S., Johnston, A. (2016) Using Species Proportions to  
371 Quantify Turnover in Biodiversity. *Journal of Agricultural, Biological, and Environmental*  
372 *Statistics* 21: 363–381.

373

374

### 375 **Supporting information**

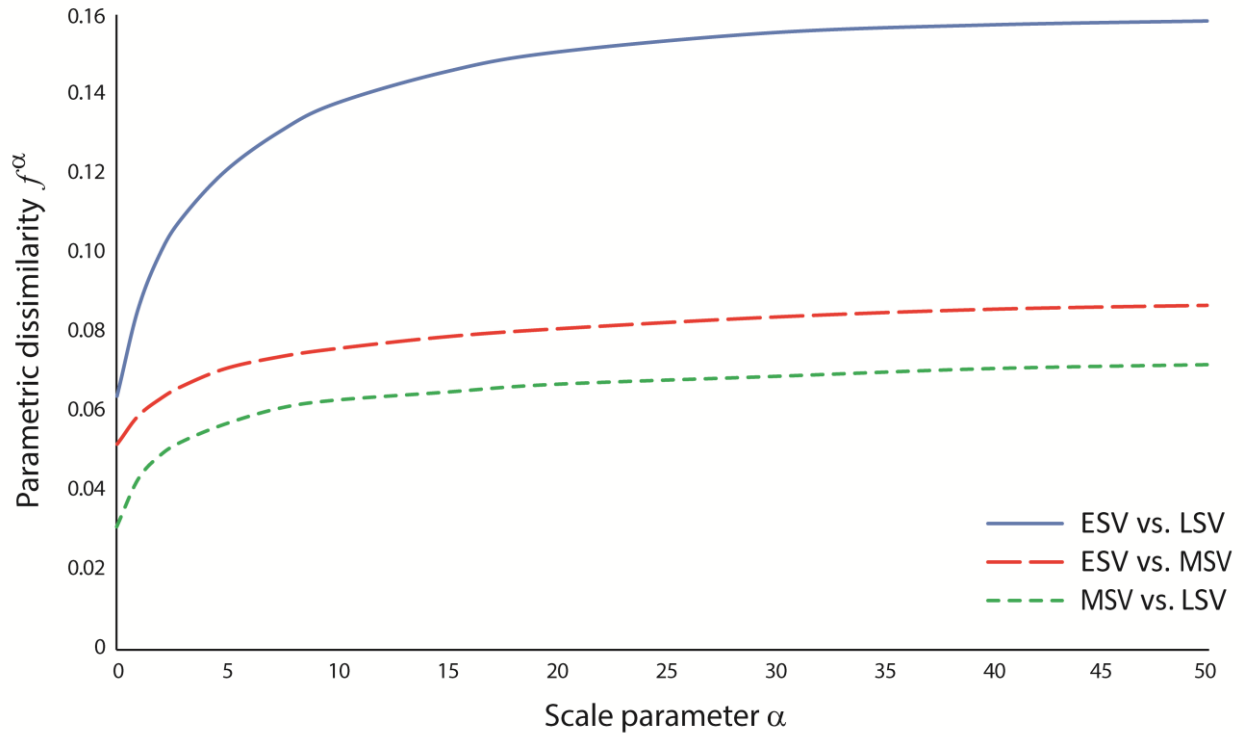
376 **Appendix 1.** R scripts for the calculation of parametric dissimilarity: manual and examples.

377 **Appendix 2.** R scripts in text format.

378 **Appendix 3.** On the relationship between the newly proposed parametric measures of community  
379 dissimilarity and a number of classical single-point measures of resemblance.

380 **Figure 1.** Functional dissimilarity profiles  $f^\alpha$  vs.  $\alpha$  among the three successional stages of the Rutor  
381 chronosequence. ESV = early successional vegetation; MSV = mid successional vegetation; LSV =  
382 late successional vegetation.

383  
384  
385  
386  
387



388